



Geophysical structural interpretation of Esh El Mellaha basin, southern Gulf of Suez: implications for oil potential in South Malak and Rabeh fields

Ahmed Elbahrawy · Mohammad A. Omran ·
Hossam Khamees · Mohammad A. Sarhan

Received: 17 November 2022 / Accepted: 11 May 2023
© The Author(s) 2023

Abstract Esh El Mellaha area is located at the western margin of the Gulf of Suez rift system. It is one of the most important potential hydrocarbon resources in the north Eastern Desert. Satellite images, field observations (e.g. measure relevant structures, lineaments mapping, compile maps at the outcrops) and seismic data were used to delineate the surface and subsurface structural elements of the area west of Esh El Mellaha range. The present study revealed that, the main structural trends have the directions NW–SE, NE–SW to NNW–SSE, WNW–ESE and ENE–WSW. The NW–SE trending faults are the major dominating trend which is related to the Gulf of Suez rift opening. The seismic interpretation step led to the identification of four prominent continuous reflectors and five depositional seismic sequences. The recognised seismic reflectors were named; Q, F, R and K and ranging in age from the Lower Miocene to the Middle–Upper Miocene. The petrophysical examination exhibits good reservoir quality for the sandstones of Matulla Formation in Rabeh and South Malak fields, southern Esh El Mellaha area. These reservoirs display low shale volume (5–20%); high effective porosity (10–20%), relatively low water saturation (40–55%) and

pay thickness varies between 30 and 85 ft. Accordingly, this study highlights the oil potentiality of the Matulla sandstones for further exploration purposes in both Rabeh and South Malak fields.

Highlights

- The main structural system controlling the Esh El Mellaha basin.
- The sandstones of Matulla Formation exhibit promising hydrocarbon reservoir in Esh El Mellaha basin.
- Future explorations in the Esh El Mellaha basin are recommended and should focus on the Matulla Formation especially in Rabeh and South Malak fields.

Keywords Esh El Mallaha · South Malak field · Rabeh field · Matulla sandstones · Seismic interpretation

1 Introduction

The Gulf of Suez basin includes over 80 fields that produce oil from Precambrian to Tertiary reservoirs. Numerous geological studies on the evolution of the Gulf of Suez basin rifting have been conducted as a result of large amounts of exploration data and the presence of well-exposed syn-rift strata (e.g. Farouk

A. Elbahrawy · M. A. Omran · M. A. Sarhan (✉)
Geology Department, Faculty of Science, Damietta
University, New Damietta City 34517, Egypt
e-mail: msarhan@du.edu.eg

H. Khamees
Egyptian Nuclear Materials Authority, Cairo, Egypt

et al. 2022, 2023; Shehata et al. 2023; Radwan, et al. 2020, 2021; Radwan and Sen 2021; Moustafa and Khalil 2020; Radwan 2021; Sarhan and Basal 2019; Sarhan 2020, 2021a, b).

Esh El Mellaha area is known as the WEEM block and is considered as one of the southwestern Gulf of Suez basin. It is located west of Gemsa field, which was productively discovered by the Egyptian Gulf of Suez Petroleum Company (EGPC 1996). The study area (WEEM block) is onshore province, which lies in southern western side of the Gulf of Suez, which is relatively a mature exploration province (Fig. 1). Esh El Mellaha basin is trending NW–SE as a part of the major Tertiary (Oligocene to Miocene) rift system (El Diasty et al. 2020). In this basin, approximately about 70% of the hydrocarbon reserves existed in the syn-rift Miocene sandstones, while most of the remaining hydrocarbons occur in the pre-rift Cretaceous and older sandstones (Pivnik et al. 2003). The WEEM area is dominated by the NW–SE trending normal faults contemporaneous to the Suez rift system and is effectively subdivided into two zones by a significant strike slip NE–SW fault transfer that is clearly visible on the surface geology at Abu Shaar Plateau (Amer et al. 2012).

Esh El Mellaha basin exhibits deep marine depositional settings; rapid sedimentation accompanied or followed the rifting system. Coeval growth faults, folds as well as transfer zones are considered as the major control on the stacking patterns and geometry of the syn-rift sediments. It displays onlap and intra-formational unconformities towards the growth monoclines and buried faults (Ghorab and Marzouk 1967). The pre-Miocene Matulla and Nubia formations, including the weathered and/or fractured basement, and the basal Miocene Nukhul sandstones (Fig. 2), are the major objectives reservoirs throughout the WEEM Block. Other potential reservoirs, as seen in the Gulf of Suez region, would be the sandstones in the overlying Kareem and Rudeis formations. Many efficient seals are present throughout the sedimentary sections. The ultimate seal for the entire petroleum system is the widespread Late Miocene evaporite sequence (Mitchell et al. 1992).

Two unconformity surfaces separate the Matulla Formation from the underlain Wata Formation and the superimposed Brown limestone Formation. The Coniacian–Santonian period saw the complete deposition of the clastics that make up the Matulla

Fm. The Matulla Fm. is characterised by a variety of planktonic foraminifera, including *D. asymetrica* and *Dicarinella concavata* zones that demonstrate the Coniacian–Santonian (Alsharhan 2003). The Coniacian–Santonian age represents a complete depositional cycle within which the Matulla Fm. was deposited. This sequence is distinguished into; low-stand systems tract (LST), transgressive systems tract (TST) and highstand systems tract (HST). The lowest portion of the Matulla Fm. deposited as LST as a result of a decrease in accommodation space near the inner shelf water-depth, while the middle section of the Matulla Fm. was deposited as TST within a comparatively deeper marine environment (outer shelf conditions). The uppermost HST was formed due to a large drop in the holding accommodation space at the final basin filling stage (Elhossainy et al. 2021a, b).

This study concludes the structural settings of Esh El Mellaha basin by the integration of seismic and remote sensing dataset. In addition, the present work assesses the petrophysical characteristics for the sandstone levels of the Matulla Formation in Rabeh and South Malak fields, southern Esh El Mellaha area.

This research sheds light on the structural background as well as the quantitative petrophysical properties, reservoir quality distribution, and hydrocarbon potential of the Matulla clastic reservoir in the examined fields which will have a great impact in reducing the risks associated with the future oil exploration in the southern Esh El Mellaha area. However, the wireline logs serve as the only applied technique used in the petrophysical assessment in this work. Accordingly, the fundamental restriction is that direct core-based measurements cannot calibrate the inferred rock parameters. The absence of routine or special core analyses is a problem that frequently arises in petrophysical evaluation projects, and it did so in our study as well.

2 Data and methods

Seismic coverage of the WEEM Block concession comprises thirty 2D seismic lines in SEG Y format (shot in 1998 by Coplex Ltd.) and, two 3D seismic surveys recorded in the southeastern portion (Fig. 1B). The available seismic data were kindly provided by the Egyptian Petroleum Authority. The acquisition parameters and the applied processing

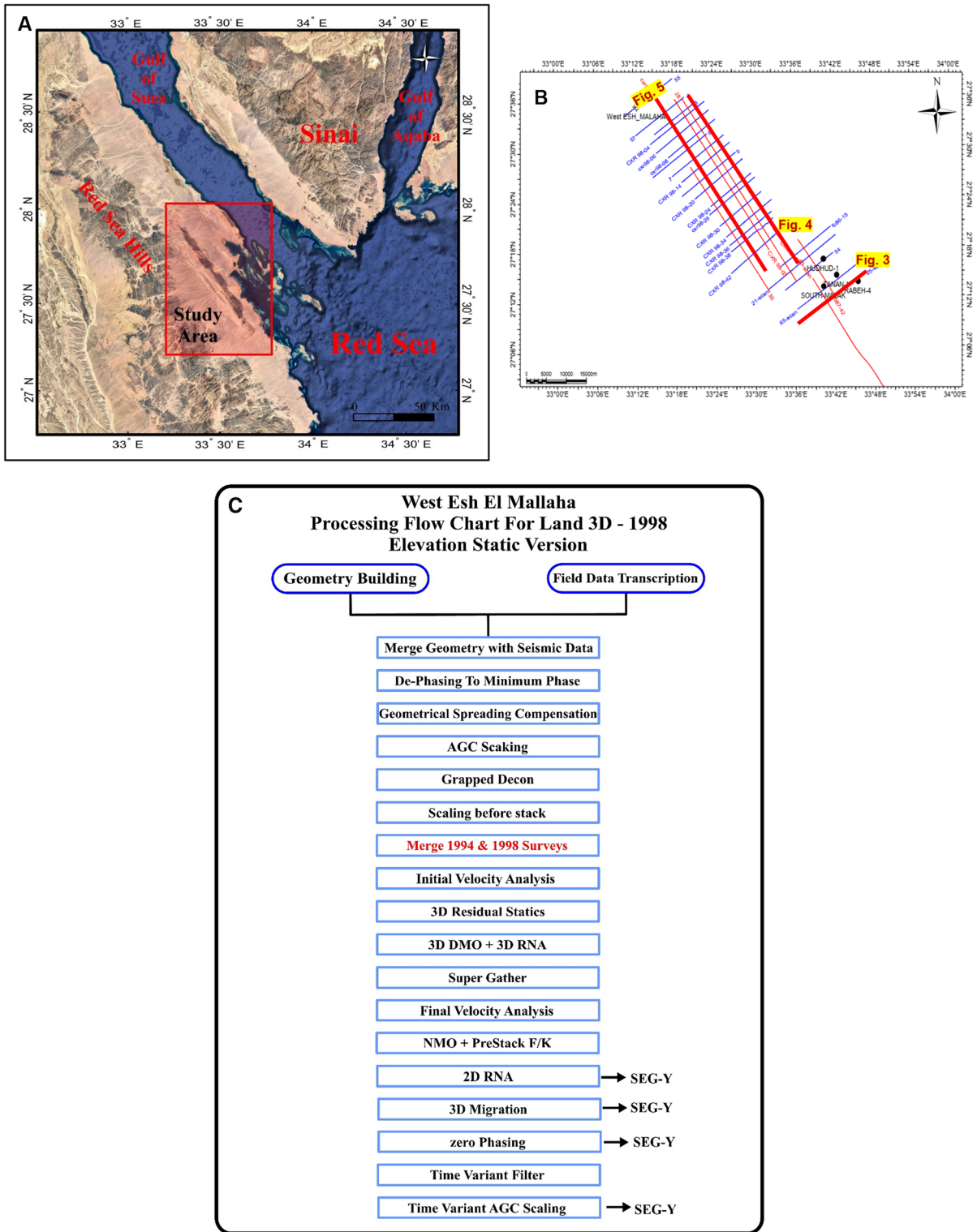


Fig. 1 **A** Aerial photo of the Gulf of Suez, Gulf of Aqaba and Northern Red Sea showing the regional framework of the study area (red rectangular). **B** Location map of the stud-

ied area including the seismic profiles and wells. **C** Flow chart summarizes the acquisition parameters and the applied processing steps on the available seismic data

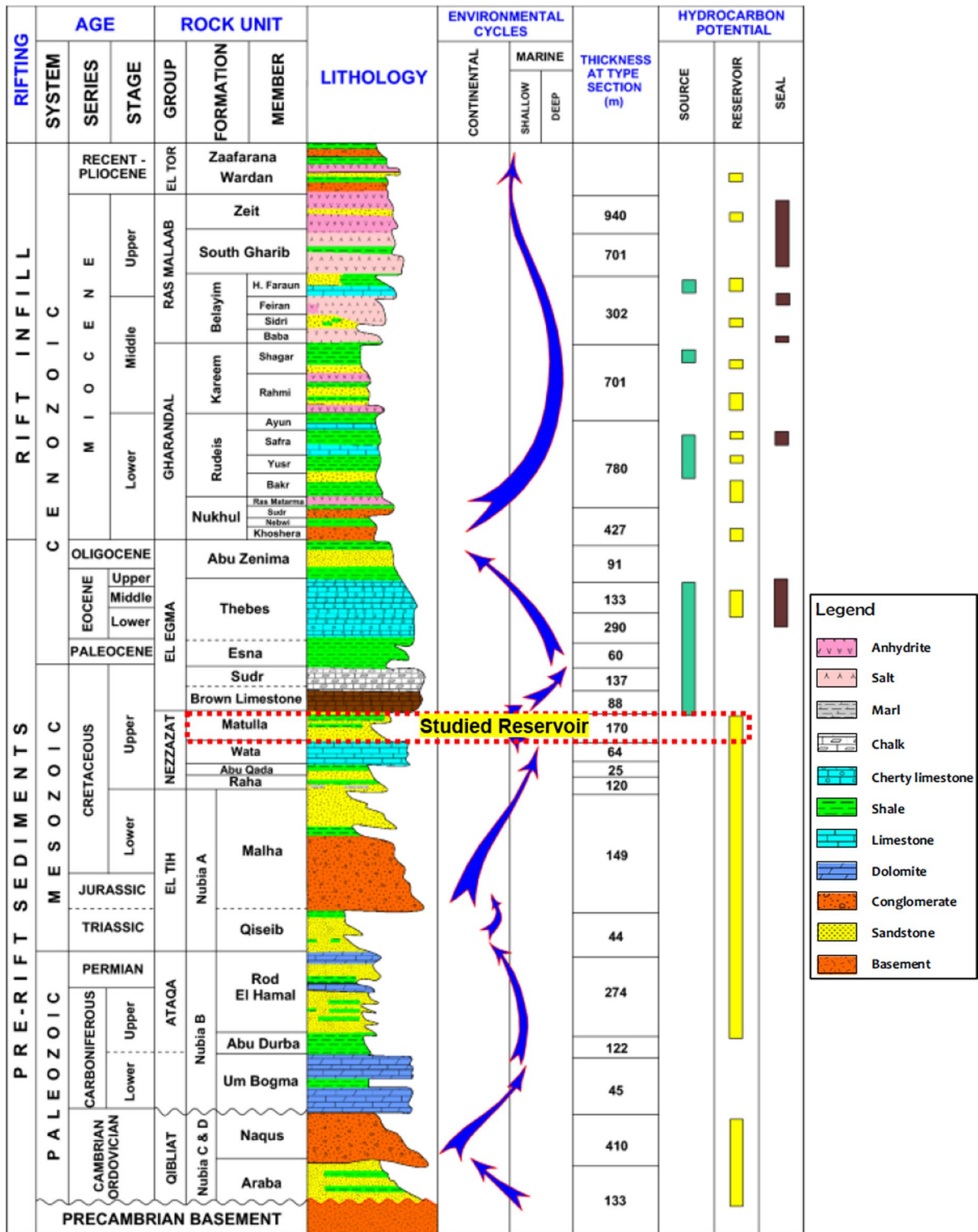


Fig. 2 General stratigraphic chart of the Gulf of Suez Basin, after El Diasty et al. (2020)

steps on this seismic data were summarized in Fig. 1C. The data includes the velocity logs for five drilled wells in the study area (Rabeh-4, South Malak-1, Hudhud-1, Tanan-1 and West Esh El Mellaha) as well as the mud logs and full conventional wire-line logs data for only two wells (Rabeh-4 well and South Malak-1 well).

The process of seismic interpretation begins with identification of the continuous prominent, high amplitude reflector by automatic picking using the PETREL software. The picked reflectors were then tied and correlated using well log data (composite and velocity logs). The well logs can help to have a useful geological overview and also to show the probable expected areas with strong reflections. Finally, the whole survey picking process should be tied together to make sure that “all intersections of the seismic lines are considered” by using a closed loop (Badely 1985). The seismic reflectors would be identified on the basis of their acoustic characters (Omran 1990). These characters comprise the continuity of seismic reflectors, geometry, attenuation, spacing, arrangement and relation between structural and sedimentary features.

Surface and field observation had done through a detailed fieldwork was carried out during several field seasons between 2015 and 2017. The field work comprises collecting measurements of different deformation pattern and structural features affected the area. The attitude and orientation of the different types of planar and linear structural fabrics (strike and dip of bedding as well as trend and plunge of lineations) were measured in the field using the Brunton Compass. The structural data were usually collected at more or less regularly spaced stations. In the areas of special interest especially where the dip and direction of bedding planes changes the gathering of data along the structural profiles were of great help. The collected field data representing linear fabric elements are subjected to structural analysis using equal area stereographic projection to define the major structural trends dominated the examined areas. Satellite imaging technique usually carried out using Regional Landsat thematic mapper was studied to manually to extract the linear features in the study area. The ARC GIS and Rock Works were used to delineate and analyses the structural linear features. The results of trend analysis of structural trends data were plotted on a rose diagram. The presence of these linear fabrics

associated with bedding is very important in deducing the directional aspects of deformations. Linear fabric elements are widely distributed in the different rock units in the study area, as it is more easily detected in the Precambrian basement rocks. The field measurements include different linear (slickenside and fold axes) and planar features (bedding planes, fault planes and fold limbs) collected from different stations distributed all over the study area.

After that, the well-log data of the available wells were qualitatively examined to delineate the oil-bearing intervals within the Matulla Formation. This step was tracked by quantitative assessment for the petrophysical properties for the favorable intervals. The considered parameters comprise; water saturation (S_w), effective porosity (Φ_E) and shale volume (V_{Sh}). The S_w for different reservoir intervals was computed by Indonesia Model (Poupon and Leveaux 1971) while, V_{Sh} , Φ_T and Φ_E parameters were calculated using the equations of Asquith and Gibson (1982).

3 Results

3.1 Seismic interpretation

3.1.1 Identification of seismic reflectors

The following is a full description for the various encountered reflectors arranged chronologically from the youngest to the oldest. Four main reflectors were identified through Rabeh-4 well, passing through 25-scan seismic line at shot point 154. Two main fault trends were detected, one of them trending NW–SE from the dip lines and the other ENE–WSW from the strike lines. The detection of the other trends in the strike lines was difficult, as they lie parallel to the main rifting trend. Low quality data reflected on the trace of the reflectors and also on the interpretation of the lines. In addition, the tracing of the reflectors was very difficult, due to the highly deformed rock units (Figs. 3, 4, 5).

3.1.2 Description of the interpreted seismic reflectors

Four regional prominent medium to strong continuous reflectors were identified, named and arranged from old to young as Q, F, R and K reflectors. Also, five seismic sequences have been identified named as:

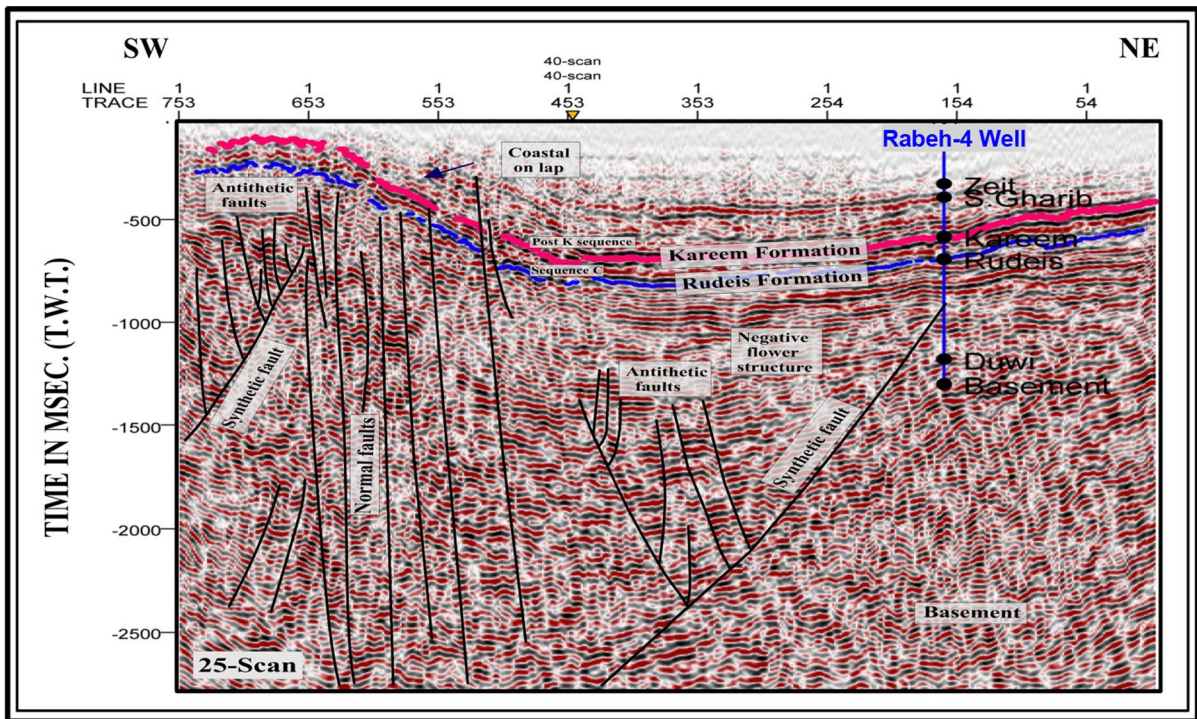


Fig. 3 Interpreted NE–SW seismic profile (no. 25-Scan) (For location see Fig. 1B)

pre Q reflector sequence, this sequence is top lapped by Q reflector, sequence A sediment bounded by reflectors Q & F, sequence B, the sequence deposited between reflectors F & R, sequence C is the unit down lapped by reflector R and top lapped by reflector K. The most recent sequence of them is named the post K reflector, which is base lapped by reflector K.

3.1.2.1 Reflector Q Reflector Q is a strong continuous, high amplitude continuous reflector extends warping the base of Esh El Mellaha basin. This reflector top lapped the rift sediments and is obstructed south east by the fault system. At the south east this reflector have been cut by normal fault represent the last rejuvenation stage of the rift system which was contemporaneous with the opening of the Gulf of Suez fault system (Figs. 3, 4, 5).

The correlation of reflector “Q” with well log data (Figs. 4, 5) indicate that it represent the lower Miocene; Rudies Formation. This reflector has medium to high amplitude appearance and represent the top of the pre-Q reflector sequence. This reflector was picked at depth ranges between 600

and 1400 ms. (t.w.t.) in most parts of the study area, which is clearly shown in line CXR 98-05. Southward, reflector Q can be picked with confidence at a depth range of 500–1200 ms (t.w.t), whereby the end of the profile, reflector Q pinches out southward probably as a consequence of the formation of a graben structure as observed between shot points 2567–2959 in the line CXR 98-38. This graben is responsible of the uplift of the sedimentary sequence south west ward. Numerous antithetic and synthetic normal faults have been observed beneath and within the sequence surrounding this reflector; probably form a rejuvenation stage of this fault system (Figs. 3, 4, 5).

3.1.2.2 Reflector F Reflector F is a medium amplitude continuous reflector which drape reflector Q upward. This reflector pinches out against reflector R at shot point 2181. This pinch is probably referred to the uplift of sedimentary sequence due to faulting and formation of the graben structure south ward. Correlation of this reflector with the well log data (Figs. 4 and 5), suggested that this boundary represents the lower–

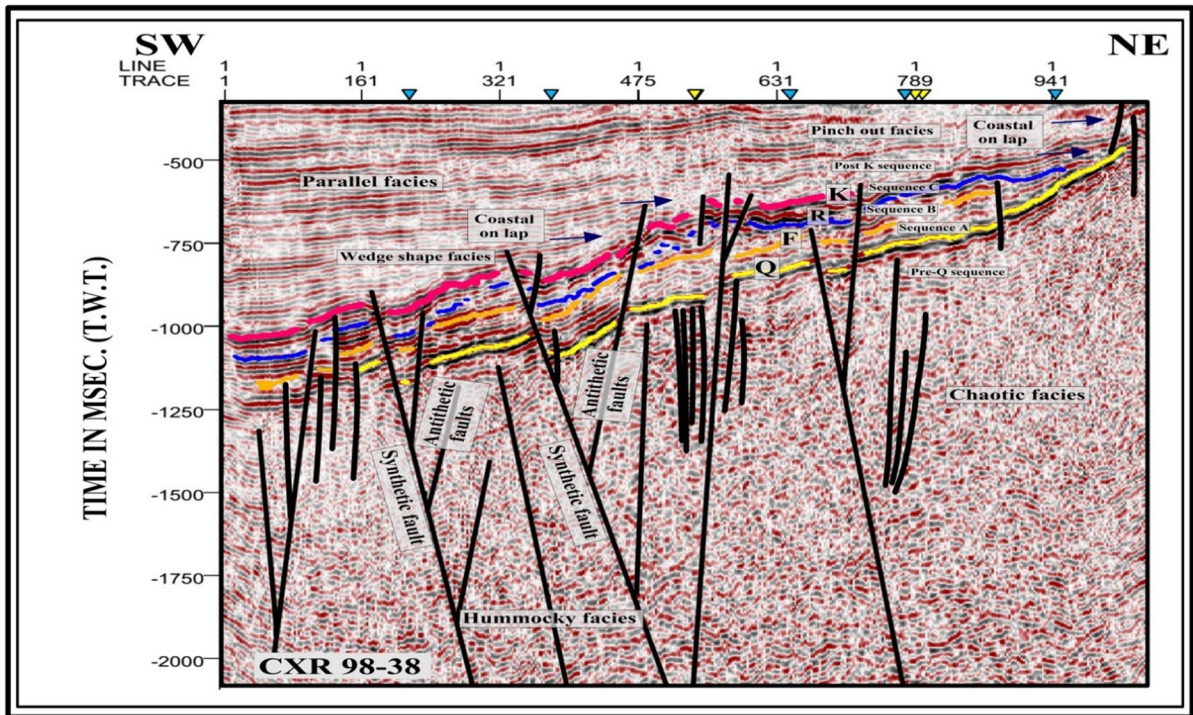


Fig. 4 Interpreted NE-SW seismic section (no. CXR 98-40) (For location see Fig. 1B)

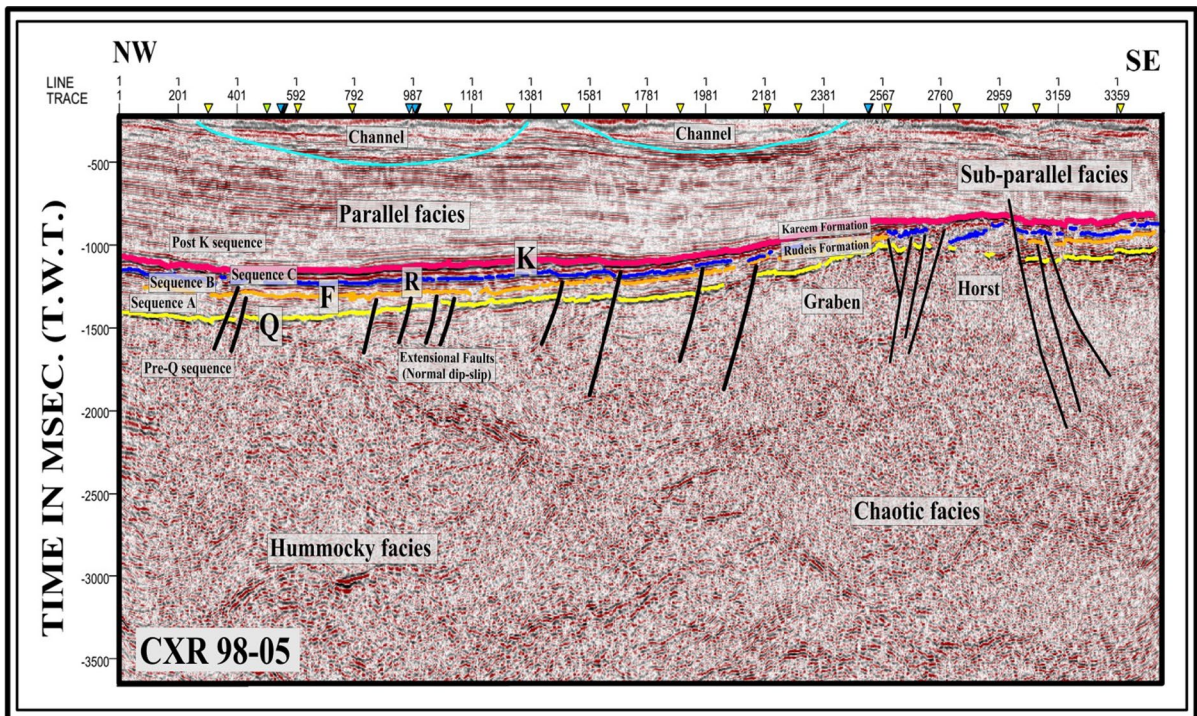


Fig. 5 Interpreted NW-SE seismic profile (no. CXR 98-05) (For location see Fig. 1B)

Middle Miocene part of Rudeis Formation, which can be picked at the basal area of the inspected area and obscured away of it due to faulting of the rift system dominated the whole area. Reflector “F” has medium amplitude and cut by different faults and can be picked at depth of 600 ms–1300 ms (t.w.t.) in most parts of the study area, as shown on line CXR 98-05 (Figs. 3, 4 and 5).

3.1.2.3 Reflector R R Reflector has a continuous to discontinuous appearance and is affected by faults. It was picked at 1100 ms (t.w.t.) in the southern part of the study area and was picked at 300 ms to about 600 ms (t.w.t.) at line 25-Scan in the northern part of the study area. This reflector is well presented in most of the study area and is overlain by parallel to sub parallel reflectors. The Reflector R indicates that it represent the Lower–Middle Miocene reflector or probably the base of Gharandal group sediments or the top of Rudies Formation (Figs. 4 and 5). It has also a medium amplitude and frequency, downlap reflector “K” forming a package of parallel facies, as observed in most of the seismic sections at the study area.

3.1.2.4 Reflector K Reflector “K” represents the upper top sequence which can be picked with confidence. It was picked at 1010 ms. (t.w.t.) at shot point 1 and at 0.6 at shot point 631 in the southern part of the study area at line CXR 98-38, and was picked from 600 ms at shot point 353–900 ms (t.w.t.) at shot point 653 in the northeastern part of the study area at line 25-Scan. Throughout the study area, it is generally dipping southwest. It continues and makes curvature, starting from shot point 553–753 at line CXR 98-05, as shown in Figs. 3, 4 and 5). This reflector can be easily picked in the examined seismic sections (Fig. 4 and 5), except for the distorted reflectors. They are characterized by medium amplitude, medium frequency and continuous to discontinuous reflectors. This reflector represents the Middle Miocene sediment or base Kareem Formation.

3.1.3 Seismic sequence analysis

The sedimentary sequence of the study area can be divided on bases of facies parameters and configuration patterns into five sedimentary sequences; these are named from base to top.

3.1.3.1 Pre-Q reflector sequence This sequence is represented by sedimentary sequence underlying reflector Q. This sequence represents the pre- Miocene sediments and is made mostly of hummocky to chaotic facies. This configuration pattern suggests that, this unit is made mainly of the pre Miocene sediment floored by basement rocks. The sequence was affected by a number faults which lead to the formation of horst and graben structures south east of the study area. Northward this sequence down lapped the sediments of Esh El Mellaha basin.

3.1.3.2 Sequence A This sequence is represented by the sediment unit bounded by reflectors Q & F. The seismic facies made sequence A is mostly form a package of parallel to sub-parallel reflectors. This pattern of formation and geometry suggests a uniform rate of deposition, as observed by the closely spaced reflectors. The wedge sediment of this sequence was terminated against a horst structure. This unit represents the lower Miocene Rudies Formation.

3.1.3.3 Sequence B This sequence represent the sediment unit bounded by reflectors F & R. Sequence B is a small wedge of parallel to sub parallel reflectors pinchs out to southern east part of the study area. The unit shows an alternation of transparent to non-transparent facies, which suggests inhomogeneity of lithologic composition. This unit displays the lower–Middle Miocene part of Rudeis formation.

3.1.3.4 Sequence C This sediment unit is bounded by reflectors R & K. This unit is made up of parallel facies with closely spaced reflector. This configuration pattern of facies suggests a uniform rate of deposition of homogenous sediments. The thickness of this unit decrease to the south east of the study area, probably due to rifting and horst formation. This unit indicates the lower middle Miocene Gharandal group.

3.1.3.5 Post K sequence This comprised the sediment sequence overlying reflector K. This sequence comprises sediment includes the formation from Kareem formation to post Zeit Formation. It ranges of age from middle Miocene to post Miocene. The sequence shows a gradual change in facies characters, directly above reflector K, a thick transparent facies is observed. Northward of the sequence parallel facies is well developed indicating an increase in sediment

supply. At the top of the sequence a channeling system is clearly observed in Figs. 3, 4 and 5.

3.1.4 Seismic structural analysis

The structural style of the picked Miocene Rudies and Kareem formations is different than the Pre-Miocene. There are major groups of faults identified from the seismic profiles as follows:

3.1.4.1 Fault system F1 This fault system consists of major synthetic faults and some minor, secondary faults, their sense of displacement is opposite to its associated major and synthetic faults (Figs. 3, 4 and 5). Antithetic-synthetic fault system is typical in areas of high normal faulting. The formation of antithetic faults confirms the rotation in the Esh El Mellaha fault block. The fault system F1 trends NNW–SSE (Gulf of Suez trend), which affects the pre-Miocene to the Miocene sequence. These faults strike approximately N 35° W and dip either to NE and SW. The irregular pattern of antithetic-synthetic faults is mainly formed due to the cross disturbance accompanied with lateral displacements parallel to the Aqaba trend.

3.1.4.2 Fault system F2 F2 fault system is the northern extension of the F1 system which has the trend of NNW–SSE (Gulf of Suez trend), which cut the pre-rift and younger sediments up to the Miocene sequence. Antithetic-synthetic fault system is the major control of the structure in this area. A major NNW–SSE trending fault dipping NE is identified. It is related to the rift bounding fault which juxtaposes the Precambrian younger granites against the Miocene and pre-Miocene sequence.

3.1.4.3 Horst–graben structures The interpretation of the seismic data indicate the occurrence of horst and graben structures as observed in Figs. 3, 4 and 5. The horst structure is identified below the uplifted area between shot point 2760–2959 at the south east of the study area. The graben structure exists to the north of the horst at shot points 2567–2381 and marks the onset of the Esh El Mellaha basin. The horst and graben structure is a common feature in the Gulf of Suez area and extended to the boundary of Esh El Mellaha basin. The triggering mechanism of the horst and graben structure is greatly attributed to the Red Sea rifting

and the opening of the Gulf of Suez and Gulf of Aqaba (e.g. Abd-Allah 2014; Amer et al. 2012; Moustafa and Khalil 2020).

3.1.4.4 Extensional fault system Extension faults are observed firming the base of Esh El Mellaha basin, it formed as step faults or an echelon type faults. These faults is greatly responsible for the subsidence of the basin floor which marked by reflector Q. The extension faults have the Gulf of Suez trend which suggests that the extension of the Esh Mellaha basin took place by the end of the Red Sea rift system.

3.1.4.5 Channels fill system Two major channel systems were observed at the top of the post k sequence. These channel played a major role in transporting the sediment infill of Esh El Mellaha basin. The time of the sediment infill was probably at the end of the middle Miocene, since the initiation of motion along the Aqaba transform fault led to a restricted subaqueous depositional environment in the Esh El Mellaha basin. The channels detected in the seismic profiles confirm that post-K sequence was deposited in a restricted basin as shown in Figs. 3, 4 and 5.

3.1.5 Mapping of the identified reflectors

Identification of the seismic boundaries or reflectors depends primarily on the contrast of their acoustic impedance contrast and consequently their reflectivity and polarity. The picked depths of seismic reflectors in two-way time were plotted on the shot point location map and contoured (Fig. 6).

3.1.5.1 Structural map of reflector K The contour map of reflector “K” (Fig. 6A) was constructed with contour interval of 350 ms (t.w.t.). The depth of reflector K in the study area ranges between 700 and 1350 ms in the eastern part. near WEEM well. It also increases toward the southern part of the study area. The depths increase gradually toward the northwestern and southern parts of the study area. The maximum value obtained is 1400 ms (t.w.t.) at the northwestern part of the map. Some closed contour lines, in the eastern and southeastern parts of these maps were noticed. The area is affected by a number of faults that have two different trends. Faults of the NW–SE trend is observed at the northwestern part of the map with a northeast throw parallel to the Gulf of Suez rifting

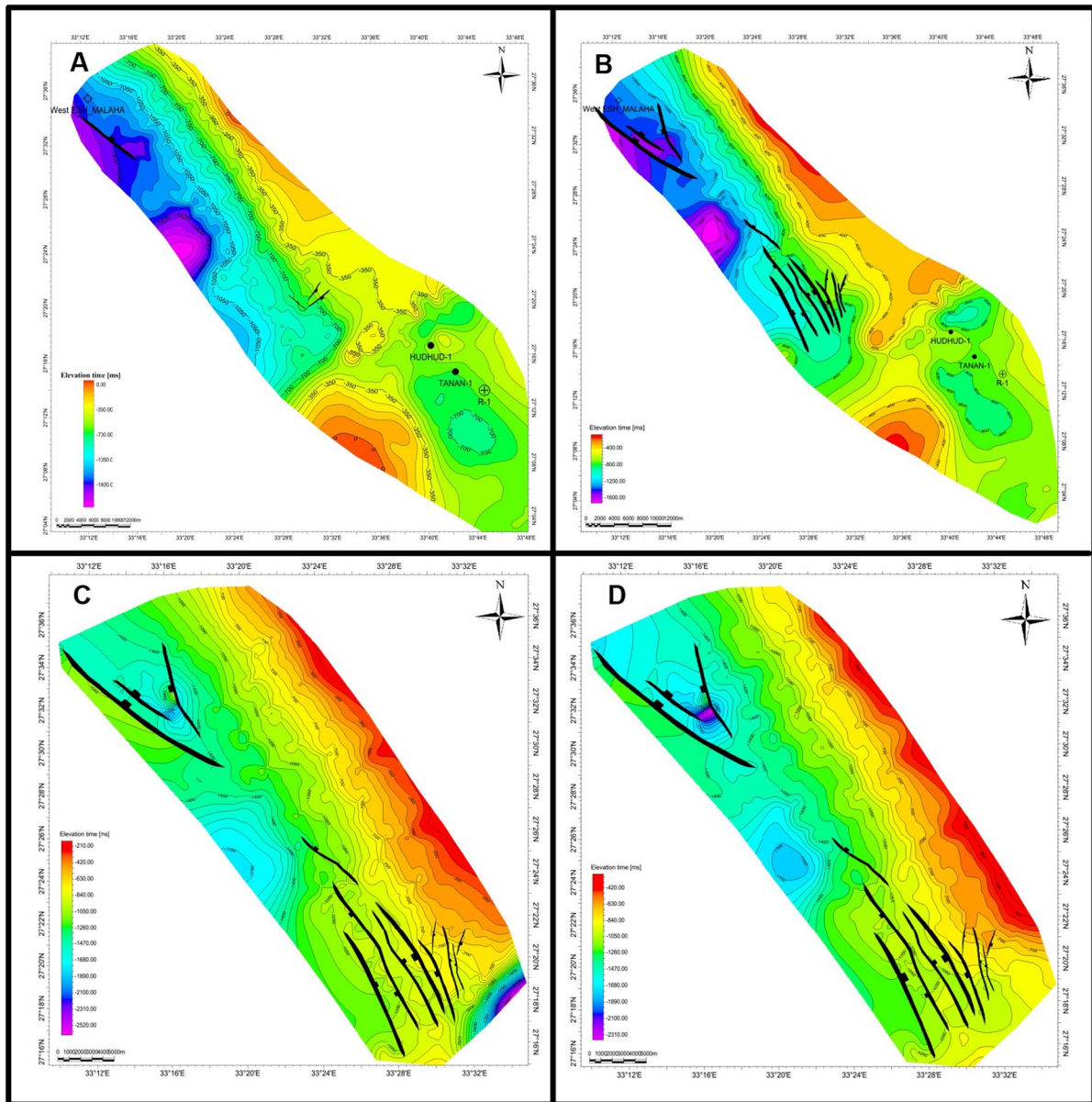


Fig. 6 Time–structural contour maps for the picked seismic reflectors in the study area. **A** Showing seismic reflector “K”. **B** Displaying seismic reflector “R”. **C** Showing seismic reflector “F”. **D** Displaying seismic reflector “Q”

trend. At the central and southern parts, another group of faults was detected trending ENE–WSW and throwing southward, which are probably related to old Precambrian cross elements.

3.1.5.2 Structural map of reflector R The structural map of reflector “R” (Fig. 6B) is constructed by using contour interval of 400 ms. It is varying in depth

between 300 and 1600 ms. The minimum depth value (350 ms) is obtained in the northeastern part of the map, while the maximum value (1600 ms) is located in the western and northwestern parts. This reflector is characterized by clear change in the depth, especially in the northwestern parts of the map and deep contours in the southeastern part. It is also affected by many faults, due to the rejuvenation of old trends and

new trends of the rifting. A new set of normal faulting is noticed in the middle part of the map, which trends in the NNW–SSE (Gulf of Suez trend) and minor synthetic NE–SW faults (Gulf of Aqaba trend). The throw of the major fault in the northwestern part is toward the northeast, while the throw of the set of faults in the middle of the map ranges from northeast to southwest “forming a highly deformed area of grabens and horsts” extended to step or extensional fault pattern.

3.1.5.3 Structural map of reflector F The contour map of reflector “F” is constructed by 350 ms contour interval (Fig. 6C). It has a depth average contour about 500 ms. The maximum value of the depth to reflector F is 1750 ms, which lies at the northwestern part of the map and at the southeastern part. The minimum depth value is 210 ms, which lies in the eastern portion of the studied area. The depth to this reflector is changed remarkably, especially in the northwestern part of the map and deep contours reaching about 2500 ms in the southeastern part. It is observed that, the number of faults affecting this reflector are greater than the number of faults affecting the two previous reflectors (K & R), which is probably attributed to the activity of the rifting processes. The faults affecting this reflector are striking in the major NW–SE rifting trend, with a northeast ward throw in the northwestern part. The faults in the southern part of the map are throwing northeast to southwest, forming a highly deformed area of grabens and horsts structures with synthetic faults trending NNE–SSW.

3.1.5.4 Structural map of reflector Q The structural map of reflector “Q” (Fig. 6D) is constructed by contour interval 350 ms, with a depth average ranging between 350 ms in the eastern part and increases toward the western part to reach 1800 ms. and also at the southern part. The depth values increase gradually toward the northwestern and southern parts of the study area. The maximum contour value is 1800 ms, which occurs in the northwestern part. In the map, closed contour lines are lying in the western and northwestern sides. This reflector is the oldest picked reflector, which is affected by many faults “due to its depth” in comparison with the other three overlying reflectors. These faults are striking in the major NW–SE rifting trend; it has a throw toward the northeast in the northwestern part. One of these faults is throwing west ward, forming a graben, where the contour values

are noticed to be higher than the other parts. In the southern part of the map, the throw ranges from the northeast to the southwest, forming a highly deformed area of grabens and horsts, with synthetic faults trending NNE–SSW.

3.2 Interpretation of surface structural trends

The results of trend analysis of the detected faults systems that affected reflectors K, R, F and Q reflectors or Kareem, Upper Rudies, Rudies and Lower Rudies formations are plotted as a rose diagram showing their trend frequencies (Fig. 7). The major trends are NNW–SSE, NW–SE, NNE–SSW and ENE–WSW, respectively, in a decreasing order. The most abundant trend is to the northwest of the normal faults and the smaller to the northeast of the shear faults (Fig. 7B). The total length frequencies of all lineations of the Kareem Formation is nearly about 2.64, while the frequencies of the other reflectors R, F and Q of the Rudies Formation are 17.8, 26.44 and 26.57, respectively. The intensity of the stresses increases “as the depth increases in the Miocene section” without remarkable change in their trends. It is not a role to increase the stresses with depth, but the stresses may increase and decrease formation-wise. This may be evidenced by the parameters of the faults.

The fracture and accordingly the fracture analysis expressions should not be used without the presence of predominantly evidence supported by the field actuality and at least about 70 percent of the linear features are controlled structurally (El-Etr 1967). This leads to confirm that, all fractures are linear, but not all-linear features are necessarily fractures (Mallard 1958), which correspond with the definition of air photo linears (Blanchet 1957; Lattman 1958).

The major trends of linear features (Fig. 8) derived from the field observations with the satellite image (Fig. 8A) are detected and analyzed. The azimuth-trend frequency rose diagram for these measurements is drawn and compared to its counterpart in the subsurface derived from the maps. The major trends are NNW–SSE, WNW–ESE, ENE–WSW, and NNE–SSW, respectively. The results of trend analysis of the structural trends data are plotted on a rose diagram (Fig. 7A).

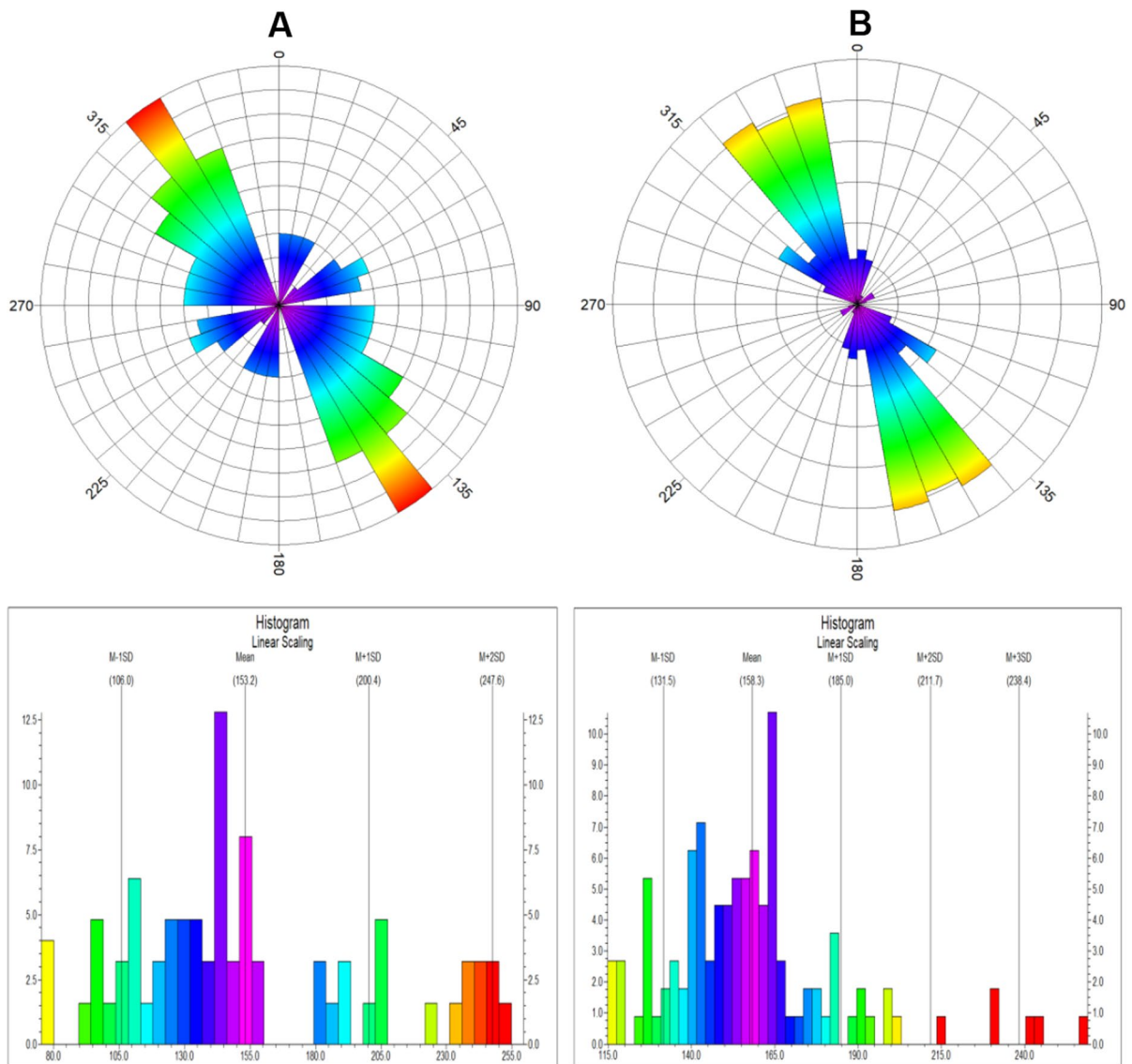


Fig. 7 Rose diagrams and histogram distribution of lineament frequencies for **A** surface field measurements and **B** subsurface detected elements

3.3 Petrophysical parameters

Based on the available mud log reports for Rabeh-4 well and South Malak-1 well, the entire sandstones of Matulla Formation comprises; colourless, tannish white, off-white, yellowish white, light brown colours, very fine to medium-grained sandstones, moderately sorted, sub-angular to sub-rounded, with kaolinite and glauconite. These previous features reflect the moderately textural maturity of Matulla

sandstones. Furthermore, these sandstones display brown to dark brown oil stains and occasionally spotty oil stain, golden yellow fluorescence and pale blue moderate stream-cut. The mud logs are also displaying high values of chromatographic gas analysis beside the attendance of oil shows opposite the uppermost sandstones of Matulla Formation in both wells.

The visual inspection of the well-log data for Matulla Formation in Rabeh-4 well reveals three pay

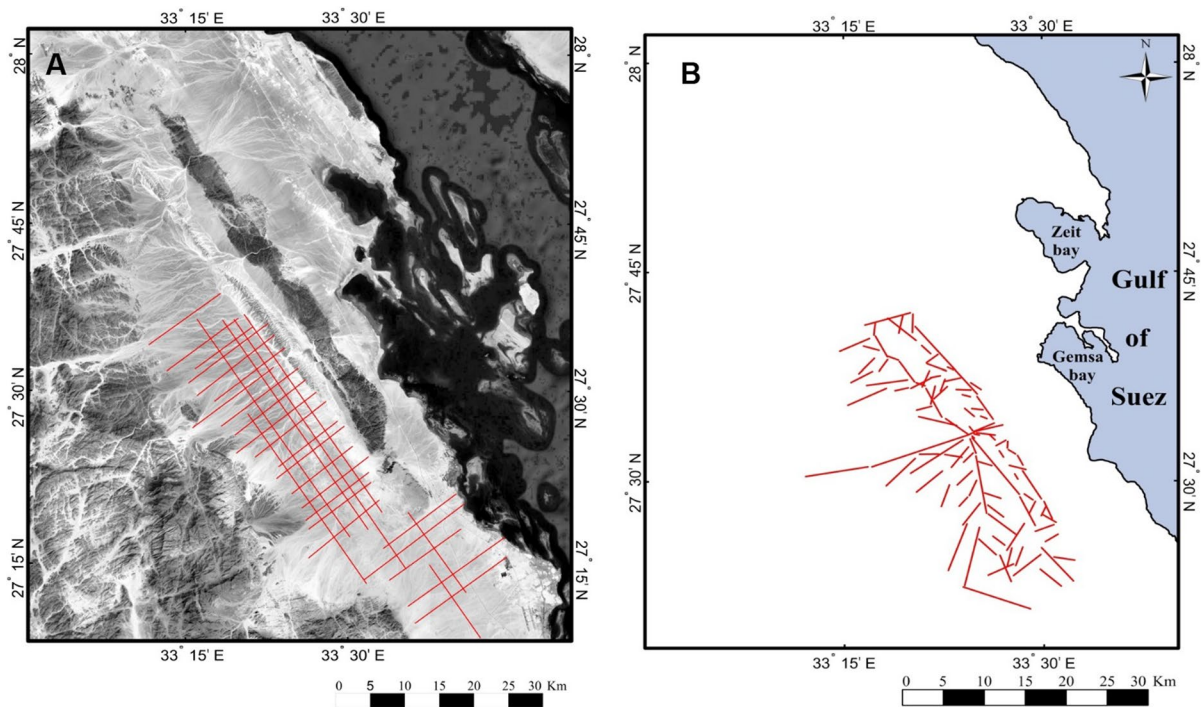


Fig. 8 **A** Enhanced satellite image showing the seismic profiles of the west Esh El Mellaha basin, Gulf of Suez, Egypt. **B** Surface lineaments map of the study area, west Esh El Mellaha basin, Gulf of Suez, Egypt

intervals locate between 5975 and 6200 ft in depth (Fig. 9). These intervals together display 85 ft thick. While the only potential zone in South Malak-1 well lies between depths of 10,870 and 10,900 ft (30 ft thick) (Fig. 9).

Numerous characteristics were used to infer the superiority of the tested intervals as potential oil reservoirs, including the low shale content as shown by the low gamma-ray log values, the high values of the deep-resistivity log, the sandy matrix, and the high porosity values of the neutron curve, (Fig. 9).

The performed petrophysical calculations in the assessed wells for the promising intervals inside Matulla Formation specify that the shale volume is usually below than 5% in Rabeh-4 well and reaches 20% in South Malak-1 well. Therefore, the effective porosity is greater in Rabeh-4 well, where values range between 15 and 25% (i.e. 20% in average), whereas, in South Malak-1 well these values vary between 5 and 15% (i.e. 10% in average).

The Neutron-Density cross-plots (Schlumberger 1972) for the three oil zones in Rabeh-4 well shows clearly the high porosity values (20–25%) with the

grouping of the plotted points close to the sandstone line (i.e., reflecting the cleaner sand with lower shale content) (Fig. 10). However, the potential reservoir interval in South Malak-1 well shows a lower porosity value (10–15%) and reveals several points clustering around and below the limestone line. This is caused by the shale effect, which led to an apparent increase in the density values of the plotted sand grains (Fig. 10).

The majority of the calculated S_w values are usually varying between 35 and 50% in Rabeh-4 well, whereas, in South Malak-1 well ranging between 40 and 60%. The constructed Pickett cross-plots (Pickett 1972) demonstrate that the majority of the points corresponding to the oil reservoirs in the examined wells should be grouped beneath the $S_w = 50\%$ line, confirming the petrophysical calculations and highlighting the significant potential of these intervals. (Fig. 11).

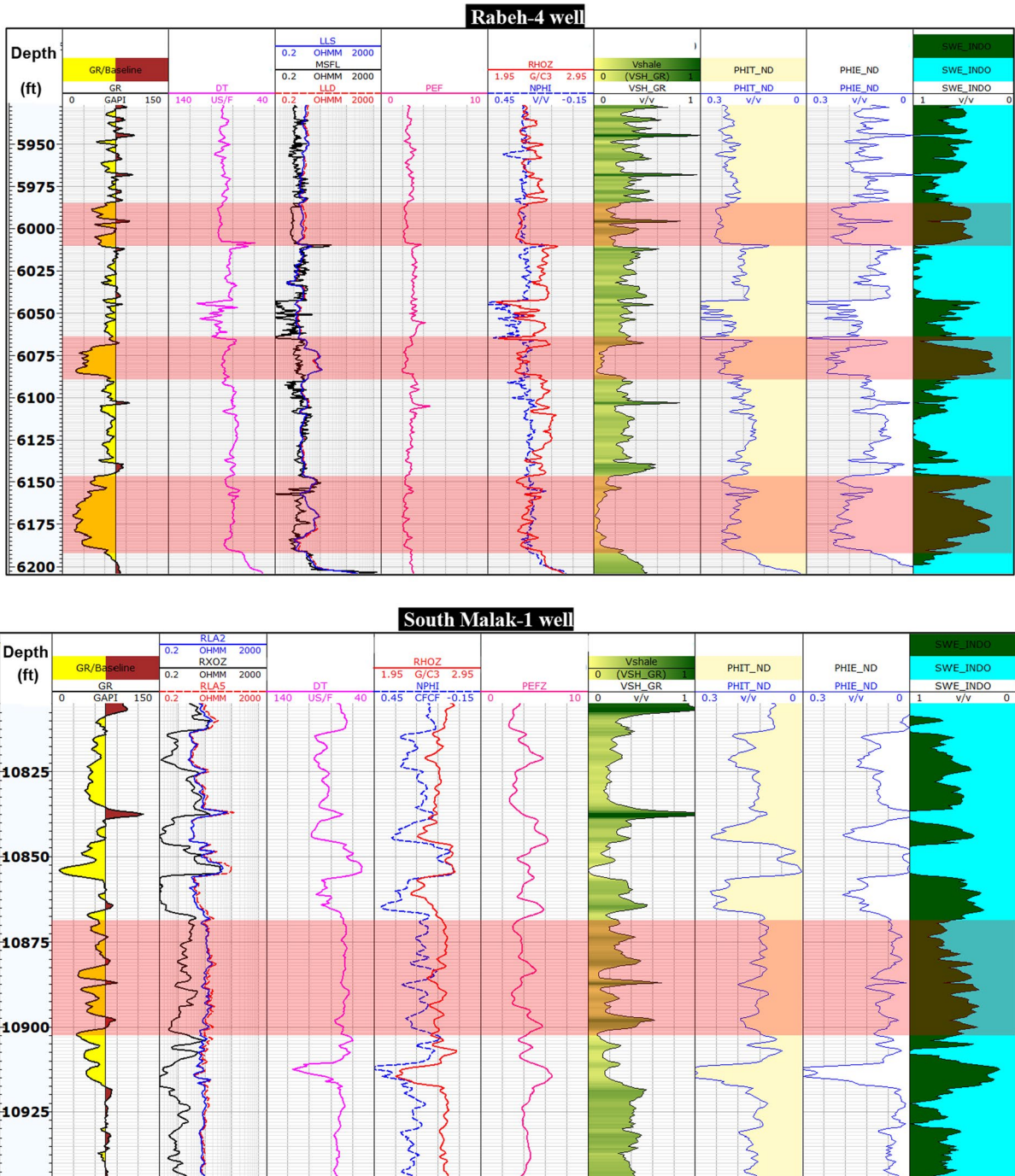


Fig. 9 Wireline logs with interpretation display the oil-pay zones within Rabeh-4 well and South Malak-1 well

4 Discussion

Structural evolution of the Esh El Mellaha basin through the interpretation of the seismic data, satellite

image analysis and surface structural observation indicated that the study area have been affected by regional tectonics. The subsurface structures comprises a major NNW–SSE trending fault system

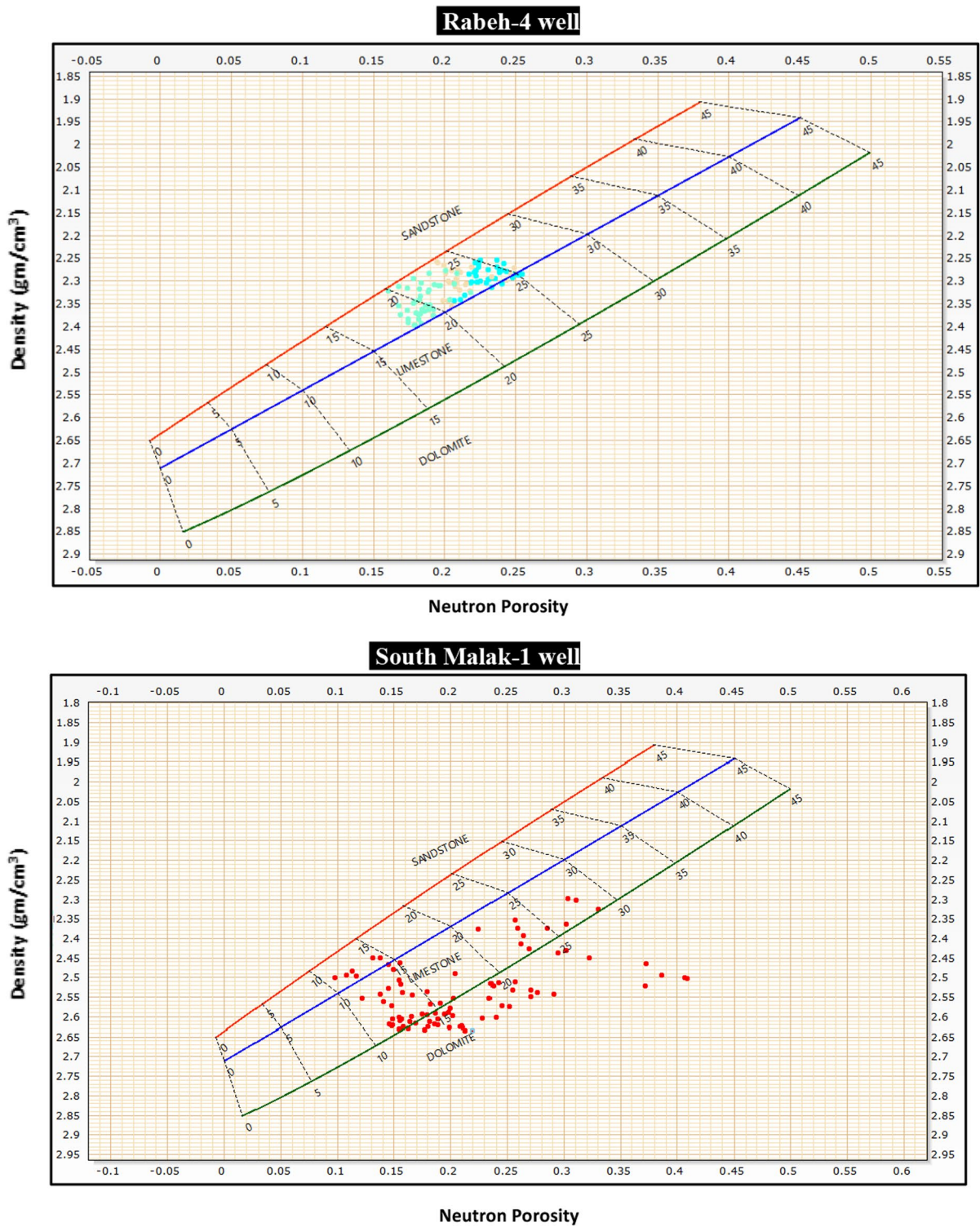


Fig. 10 Neutron–Density cross-plots for the oil zones within Rabeh-4 well and South Malak-1 well

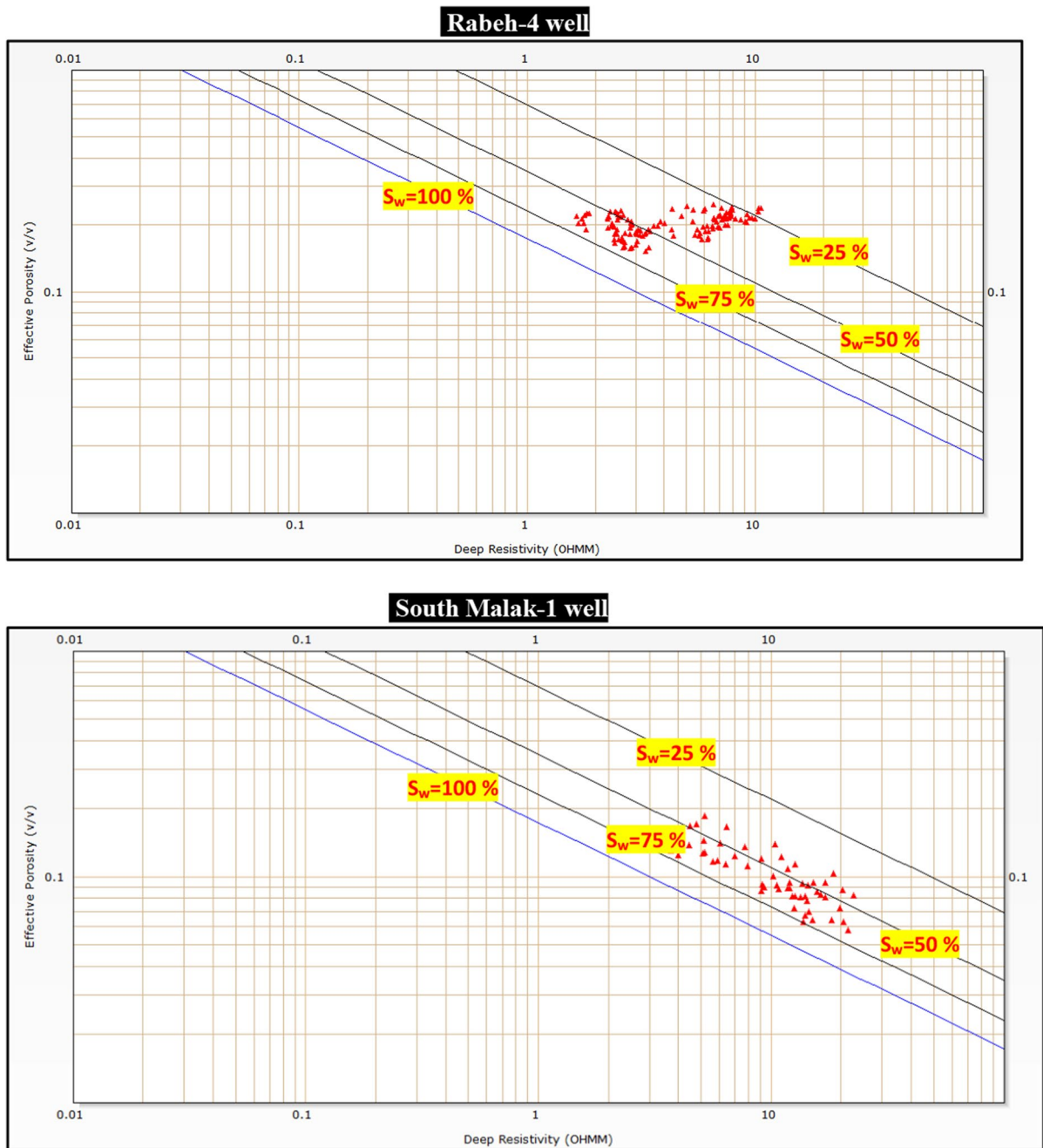


Fig. 11 Pickett cross-plots for the reservoir intervals within Rabeh-4 well and South Malak-1 well

which is dipping NE and SW which form a group of horsts and grabens in the basin. Esh El Mellaha basin is bounded by NNW–SSE rift bounding faults which bring the basement against the younger pre-Miocene and Miocene sediments.

Using the geophysical studies on Esh El Mellaha area using magnetic methods and gamma spectrometric, Khalil (1992) concluded that the area has two major high anomalies which affected by two sets of faults one of them trending ENE–NE and the other one is trending NNW. The uplift occurred during

the late Miocene, caused movements along the fault planes in the dip direction, which formed the oblique type faulting (Abu El-Ata and Helal 1992). The Gulf of Suez evolution model proposed by Omran (1995) deduced that the Gulf of Suez trend is considered as a right-lateral direction which has been rejuvenated periodically, but mainly during the Hercynian and Alpine (Laramide and Syrian) orogenies. This trend is considered to be the principal controlling direction in the Red Sea–Gulf of Suez Rift system. The subsurface interpretation from aeromagnetic data using the Euler method with integration of observed field data of Esh El Mellaha area resulted that the area is dissected by a system of faults striking in the NW direction (Aboud et al. 2004).

According to Hammed (2002) four fault trends were recorded in Esh El Mellaha area. The Gulf parallel or Clysmic fault trend (NNW–NW), the E-to ENE- cross trend, the Duwi N 75 W trend and the Aqaba NNE-trend. Field study and the paleostress analysis were carried out, which resulted that four Late Tertiary rifting phases affected Esh El Mellaha area. The rotation of the pre-rift rocks throughout the rifting phase caused the syn-rift rocks rest in the structural low areas of the pre-rift units. Esh El Mellaha block was a relatively uplifted block. It was uplifted after the depositional process of the Miocene Rudies Formation and represented as the western rift shoulder for a deep marine basin eastward (Abd-Allah et al. 2014).

The surface field study in this work indicated that the major fault trends recorded in the study area are NNW–SSE Gulf parallel trend, ENE–WSW old Precambrian cross faults and NNE–SSW Aqaba trend, while the Duwi trend is not detected.

The results of the present work showed that, the Esh El Mellaha area is dissected by a system of faults. It is controlled mainly by major faults striking NNW–SSE to NW–SE direction, with down thrown to the southeast and some are throwing southwest, which in turns form horst and graben structure. This trend is directly related to the Clysmic fault trend which is a Gulf parallel fault trending approximately N 35° W.

These structural elements are related to the Gulf of Suez rift system. The study area is characterized mainly by the presence of main structural trends NW–SE and NNW–SSE the rifting fault trend

and Aqaba NNE–SSW trend, which are dissected by the cross elements expressed by shear faults trending ENE–WSW (old Precambrian cross fault trend), that are perpendicular to the major Clysmic trend of the rifting.

The sandstones of the Matulla Formation in Rabeh and South Malak fields, southern Esh El Mellaha area are potential oil reservoir in the study area. In Rabeh field, the effective porosity is 20%, water saturation is 40% and the total net pay zones thickness is 85 feet. While, in South Malak field, the effective porosity is 10%, water saturation is 55% with 30 ft net pay thick. Accordingly, the current study emphasised the oil potentiality of the Matulla sandstones for future development and exploration processes in Esh El Mellaha basin.

5 Conclusions

- The main structural system controlling the area is trending NW–SE and NNW–SSE which are related to the Clysmic event (the rifting initiation).
- Another NNE–SSW trending system is affecting the study area, which represents the Aqaba-dead sea transform trend.
- The cross elements dissecting the major trends are shearing faults trending ENE-WSW, which is related to the old Precambrian cross fault trend.
- Esh El Mellaha block was uplifted during the middle to late Miocene post kareem Formation.
- The western rift shoulder is trending NNW–SSE and dipping eastward, where deep marine sediments which deposited to the east of the rift shoulder are in faulted against the Precambrian rock units.
- The sandstones of Matulla Formation exhibit promising hydrocarbon reservoir in Esh El Mellaha basin.
- The reservoir intervals within Matulla sandstones display valuable capability for good reservoirs conditions with thicknesses varies within 30–85 ft range; effective porosity between 10 and 20%; shale volume between 5 and 20%; and water saturation ranges between 40 and 55%.
- According to these findings, future explorations in the Esh El Mellaha basin are recommended

and should focus on the Matulla Formation especially in Rabeh and South Malak fields

Acknowledgements The authors would like to thank the Egyptian General Petroleum cooperation (EGPC) and Ganoub El Wadi Holding Petroleum Company for the permission to use the seismic data needed for conducting this work.

Author contributions All authors have contributed equally.

Funding Open access funding provided by The Science, Technology & Innovation Funding Authority (STDF) in cooperation with The Egyptian Knowledge Bank (EKB). No funding available for this study.

Data availability The geophysical data in the present work is confidential.

Declarations

Competing interests Here, we authorize that there is no conflict of interest.

Consent to publish Here, we give our consent for the present manuscript to be published in this journal after the acceptance.

Ethical statement We certify that this manuscript reflects our own research and has never been published before and not being considered for publication anywhere.

Open Access This article is licensed under a Creative Commons Attribution 4.0 International License, which permits use, sharing, adaptation, distribution and reproduction in any medium or format, as long as you give appropriate credit to the original author(s) and the source, provide a link to the Creative Commons licence, and indicate if changes were made. The images or other third party material in this article are included in the article's Creative Commons licence, unless indicated otherwise in a credit line to the material. If material is not included in the article's Creative Commons licence and your intended use is not permitted by statutory regulation or exceeds the permitted use, you will need to obtain permission directly from the copyright holder. To view a copy of this licence, visit <http://creativecommons.org/licenses/by/4.0/>.

References

- Abd-Allah AMA (2014) Structural evolution of the southern transfer zone of the Gulf of Suez rift, Egypt. *J Afr Earth Sci* 96:21–38
- About E, Salem A, Ushijima K (2004) Structural imaging of Esh El Mallaha area, Gulf of Suez, Egypt using Euler method, ASEG Geophysical Conference and Exhibition, Sydney, vol 17
- Abu El-Ata ASA, Helal AA (1992) The potential of the seismic interpretation in delineating the shearing deformations and their tectonic implications along the western coast of the Gulf of Suez, Egypt. *Ann Geol Survey Egypt* 18:249–266
- Alsharhan AS (2003) Petroleum geology and potential hydrocarbon plays in the Gulf of Suez rift basin, Egypt. *AAPG Bull* 87(1):143–180
- Amer R, Sultan M, Ripperdan R, Encarnación J (2012) Structural architecture for development of marginal extensional sub-basins in the Red Sea Active Rift Zone. *Int J Geosci* 3:133–152
- Asquith G, Gibson C (1982) Basic well log analysis for geologists: methods in Exploration series. AAPG, Tulsa, Oklahoma
- Badely M (1985) Practical seismic interpretation. International Human Resources Development Corporation, Prentice Hall, Boston
- Blanchet PH (1957) Development of fracture analysis as an exploration method. *Am Assoc Pet Geol Bull* 4:748–759
- EGPC, Egyptian General Petroleum Corporation (1996) Gulf of Suez oil fields (A comprehensive overview). EGPC, 736
- El Diasty WS, El Beialy SY, Mostafa AR, Abo Ghonaim AA, Peters KE (2020) Chemometric differentiation of oil families and their potential source rocks in the Gulf of Suez. *Nat Resour Res* 29(3):2063–2102
- El Etr HA (1967) The technique of lineation and linear analysis and its application in the mineralogenic province of south-east Missouri. [Ph.D. Thesis], University of Missouri at Rolla USA
- Elhossainy MM, Salman AM, Sarhan MA, Al-Areeq NM, Alrefaee HA (2021a) Sequence stratigraphic analysis and depositional evolution of the upper cretaceous deposits in Ras Budran oil field, Gulf of Suez, Egypt. *Arab J Geosci* 14(12):1–13
- Elhossainy MM, Salman AM, Sarhan MA, Al-Areeq NM, Alrefaee HA (2021b) Sequence stratigraphic analysis and depositional evolution of the upper cretaceous deposits in Ras Budran oil field, Gulf of Suez, Egypt. *Arab J Geosci* 14(12):1104
- Farouk S, Sen S, Pigott JD, Sarhan MA (2022) Reservoir characterization of the middle Miocene Kareem sandstones, Southern Gulf of Suez Basin, Egypt. *Geomech Geophys Geo-Energy Geo-Resour* 8(5):130
- Farouk S, Sen S, Belal N, Omran MA, Assal EM, Sarhan MA (2023) Assessment of the petrophysical properties and hydrocarbon potential of the lower Miocene Nukhul formation in the Abu Rudeis-Sidri Field, Gulf of Suez Basin, Egypt. *Geomech Geophys Geo-Energy Geo-Resour* 9(1):36
- Ghorab MA, Marzouk IM (1967) A summary report on the rock-stratigraphic classification of the Miocene non-marine and coastal facies in the Gulf of Suez and Red Sea Coast. General Petroleum Company, Cairo, UN Published report, E.R. p 601
- Hammed MSH (2002) Geology and structural architecture of southwest Gulf of Suez, with special emphasis on the Precambrian rocks of Gebel El Zeit area, Egypt. [Ph.D.

- Thesis], The Department of Geology, Faculty of Science, Cairo University, Egypt
- Khalil AF (1992) Use of airborne spectrometric and magnetic survey data in the exploration of radioactive occurrences in Bir Mellaha area, North Eastern Desert, Egypt, Scientific international report series, Nuclear materials authority, Cairo, Egypt, p 17
- Lattman LH (1958) Technique of mapping geologic fracture traces and lineaments on aerial photographs. *Photogramm Eng* 24:568–576
- Mallard JD (1958) Photogeophysics its application in petroleum exploration over the glaciated plains of western Canada. In: The 2nd Williston basin conference Proc. Conrad. Publ. co. Bismark, North Dakota
- Mitchell DJW, Allen RB, Salama W, Abouzakm A (1992) Tectonostratigraphic framework and hydrocarbon potential of the Red Sea. *J Pet Geol* 15:187–210
- Moustafa AR, Khalil SM (2020) Structural setting and tectonic evolution of the Gulf of Suez, NW Red Sea and Gulf of Aqaba Rift Systems. In: The geology of Egypt, Springer, Cham, pp 295–342
- Omran MA (1990) Geophysical studies in the Hebrides terrace seamount, NE. Atlantic. [Ph.D. Thesis], University of Wales, UK
- Omran MA (1995) Structural evolution of the central Gulf of Suez area from seismic data. *Afr Geosci Rev* 2(1):153–168
- Pickett GR (1972) Practical Fm. evaluation. Golden, Colorado, G.R. Pickett, Inc.
- Pivnik DA, Ramzy M, Steer BL, Thorseth J, El Sisi Z, Gaafar I, Garing JD, Tucker RS (2003) Episodic growth of normal faults as recorded by syntectonic sediments, July oil field, Suez rift, Egypt. *AAPG Bull* 87(6):1015–1030
- Poupon A, Leveaux J (1971) Evaluation of water saturation in shaly formations. In: SPWLA 12th annual logging symposium. Society of Petrophysicists and Well-Log Analysts
- Radwan AE (2021) Modeling pore pressure and fracture pressure using integrated well logging, drilling based interpretations and reservoir data in the giant El Morgan oil field, Gulf of Suez, Egypt. *J Afr Earth Sci* 178:104165
- Radwan AE, Kassem AA, Kassem A (2020) Radwany Formation: a new formation name for the Early-Middle Eocene carbonate sediments of the offshore October oil field, Gulf of Suez: contribution to the Eocene sediments in Egypt. *Mar Pet Geol* 116:104304
- Radwan AE, Rohais S, Chiarella D (2021) Combined stratigraphic-structural play characterization in hydrocarbon exploration: a case study of middle Miocene sandstones, Gulf of Suez basin, Egypt. *J Asian Earth Sci* 218:104686
- Radwan A, Sen S (2021) Stress path analysis for characterization of in situ stress state and effect of reservoir depletion on present-day stress magnitudes: reservoir geomechanical modeling in the Gulf of Suez Rift Basin, Egypt. *Nat Resour Res* 30(1):463–478
- Sarhan MA (2020) Geophysical appraisal and oil potential for Rudeis formation at West Hurghada area, southern Gulf of Suez: detection of stratigraphic trap. *Arab J Geosci* 13(6):1–9
- Sarhan MA (2021a) Geophysical and hydrocarbon prospect evaluation of Nukhul formation at Rabeh East oil field, Southern Gulf of Suez Basin, Egypt. *J Pet Explor Prod Technol* 11(7):2877–2890
- Sarhan MA (2021b) Petrophysical characterization for Thebes and Mutulla reservoirs in Rabeh East Field, Gulf of Suez Basin, via well logging interpretation. *J Pet Explor Prod Technol* 11(10):3699–3712
- Sarhan MA, Basal AMK (2019) Evaluation of Nubia sandstone reservoir as inferred from well logging data interpretation for Rabeh East-25 well, Southwest Gulf of Suez, Egypt. *J Afr Earth Sci* 155:124–136
- Schlumberger (1972) Log interpretation/charts, Houston, Schlumberger Well Services, Inc.
- Shehata AA, Tahoun SS, Kassem AA, Abdelsamea EG, Hassan HF (2023) Palynostratigraphy and paleoenvironmental inferences of the Jurassic successions, Darag Basin, Gulf of Suez, Egypt. *J Afr Earth Sci* 200:104890

Publisher's Note Springer Nature remains neutral with regard to jurisdictional claims in published maps and institutional affiliations.